in a distorted octahedral environment.[19] The third component of rhombic Os(III) spectra occurs at high field and is often unobserved. This supports the Os(III)-DBCat charge distribution and further illustrates the difference between Ru and Os in these complexes.

Spectroelectrochemistry. Spectroelectrochemical experiments were performed on $Os(bpy)_2(DBCat)$ in acetonitrile for the reversible first and second oxidation processes. Spectra are shown in Figure 5. Upon one-electron oxidation of the neutral complex, MLCT bands at 604, 510, and 442 nm disappear and new bands at 2300, 873, and 536 nm appear for the complex cation. Further one-electron oxidation results in the appearance of a new band at 558 nm and an increase in intensity for the band at 2360 nm.

The near-infrared absorption at 2300 nm observed for both $[Os(bpy)_2(DBCat)]^+$ and $[Os(bpy)_2(DBSQ)]^{2+}$ is tentatively assigned as a $d\pi$-$d\pi$ transition between levels that arise from the effects of spin-orbit coupling for Os(III).[19] Other absorptions bands of $[Os(bpy)_2(DBCat)]^+$ that appear at 536 and 873 nm may be assigned as $\pi(bpy) \rightarrow Os(III)$ and $\pi(DBCat) \rightarrow Os(III)$ LMCT bands, respectively. The band at 873 nm moves to higher energy when DBCat is replaced by Cl_4Cat, which is in accord with the positive shift in oxidation potential for the catecholate. The band at 558 nm for $[Os(bpy)_2(DBSQ)]^{2+}$ is tentatively assigned as a $\pi(DBSQ) \rightarrow Os(III)$ LMCT transition. Studies are in progress to provide further information on spectral assignments.

Discussion

The structural and spectroscopic properties of $[Ru(bpy)_2(DBSQ)]^+$ and $[Os(bpy)_2(DBCat)]^+$ indicate a subtle change in charge distribution for the complexes of second- and third-row metals. Carbon-oxygen bond lengths of the quinone ligand of the osmium complex indicate that it is a reduced catecholate, and the near-infrared transitions and rhombic EPR spectrum are indicative of Os(III). The properties of the ruthenium complex indicate that its electronic structure is best described as a mix of Ru(II)-DBSQ and Ru(III)-DBCat localized-charge forms. The comparative electrochemical properties of the Ru and Os complexes prepared with all three quinone ligands fail to show shifts in potential that would indicate that redox processes are either metal or ligand localized. The conclusion from this analysis is that the ground-state electronic structures of both the Ru and Os complexes contain weighted contributions of both quinone ligand and metal, but that the ligand orbital contribution is significantly less for osmium than ruthenium.

Acknowledgment. Research carried out at the University of Colorado was supported by the National Science Foundation under Grant CHE 88-09923. The work at Mie University was supported, in part, by the Joint Studies Program (1987-1988) of the Institute for Molecular Science, Okazaki, Japan. M.H. thanks Prof. Takeko Matsumura-Inoue at Nara University of Education for helpful discussions.

Supplementary Material Available: Tables giving electronic spectral data, crystal data and details of the structure determination, bond distances and angles, atom coordinates, anisotropic thermal parameters, and hydrogen atom parameters for $[Os(bpy)_2(DBCat)](ClO_4)$ (9 pages); a table of structure factors for $[Os(bpy)_2(DBCat)](ClO_4)$ (17 pages). Ordering information is given on any current masthead page.

Contribution from Anorganische Chemie III, Eduard-Zintl-Institut der Technischen Hochschule Darmstadt, D-6100 Darmstadt, Federal Republic of Germany, and Fachbereich Chemie, Philipps-Universität, D-3500 Marburg, Federal Republic of Germany

Spectroscopic and Kinetic Investigation of Bis(*N*-alkylsalicylaldiminato)copper(II) Complexes: A Study on the Existence of Planar ⇌ Tetrahedral Configuration Equilibria

Rainer Knoch,[1a] Andreas Wilk,[1b] Klaus J. Wannowius,[1a] Dirk Reinen,*[1b] and Horst Elias*[1a]

Received September 21, 1989

For several bis(*N*-alkylsalicylaldiminato)copper(II) complexes $Cu(R\text{-}sal)_2$ with R = methyl (I), ethyl (II), *n*-propyl (III), isopropyl (IV), neopentyl (V), 2,4-dimethylpentyl (VI), and *tert*-butyl (VII), a spectroscopic and kinetic study on the existence of configurational equilibria of the type planar ⇌ tetrahedral was carried out. It follows from the analysis of the EPR and ligand field spectra taken for the solid state, frozen solutions, and acetone solutions that, depending on the structural properties of the organic group R, the N_2O_2 coordination geometry around the copper ranges from planar to close to tetrahedral. The main conclusions derived from the spectroscopic results are as follows: (i) neither for the solid state nor for acetone solutions is an indication of a fluxional behavior in the sense of an equilibrium planar ⇌ tetrahedral found; (ii) in the solid state the angle O-Cu-O (obtained from structural data) follows the sequence I, V (180°) > VI (163°) > II (155°) > VII (142°) > IV (138°); (iii) in acetone solution the sequence is I, II, V, VI (≈155°) > IV (≈150°) > VII (≈140°); (iv) the degree of α- and/or β-branching in the alkyl group R controls the degree of nonfluxional distortion found. Visible spectrophotometry was used to study the reaction $Cu(R\text{-}sal)_2 + H_2salen \rightarrow Cu(salen) + 2R\text{-}salH$ in acetone at 298 K under pseudo-first-order conditions ($[H_2salen]_0 \gg [Cu(R\text{-}sal)_2]_0$; H_2salen = *N*,*N*′-disalicylideneethylenediamine). The kinetic data follow a two-term rate law, rate = $(k_S + k_L[H_2salen])[complex]$, with k_S ranging from 3.8×10^{-3} (I) to 0.18×10^{-3} s^{-1} V) and k_L ranging from 17×10^{-2} (I) to 0.095×10^{-2} M^{-1} s^{-1} (V). The size of second-order rate constant k_L, which can be interpreted as describing an associatively controlled ligand substitution, reflects the steric accessibility of the copper in $Cu(R\text{-}sal)_2$ rather than the degree of distortion of the CuN_2O_2 polyhedron. The kinetic results are in line with the spectroscopic findings in the sense that there is no indication of a dynamic equilibrium planar ⇌ tetrahedral for complexes $Cu(R\text{-}sal)_2$.

Introduction

The stereochemical variability and flexibility of bis(*N*-alkylsalicylaldiminato)metal(II) complexes $M(R\text{-}sal)_2$ have been the subject of numerous investigations.[2,3] Complexes $Zn(R\text{-}sal)_2$[3,4] and $Co(R\text{-}sal)_2$[3] prefer tetrahedral N_2O_2 coordination, whereas the coordination geometry of complexes $Ni(R\text{-}sal)_2$ and $Cu(R\text{-}sal)_2$ is basically of the planar *trans*-N_2O_2 type, as long as the steric demands of the organic group R are small enough.[3] Bulky groups (such as R = *tert*-butyl), however, enforce more or less strong tetrahedral distortion.

A very interesting property of the nickel complexes $Ni(R\text{-}sal)_2$ is their fast configurational isomerism in solution according to

(1) (a) Technische Hochschule Darmstadt. (b) Philipps-Universität Marburg.
(2) Holm, R. H.; Everett, G. W.; Chakravorty, A. *Progss in Inorganic Chemistry*; Interscience: New York, 1966; Vol. 7, p 83.
(3) Holm, R. H.; O'Connor, M. J. *Progss in Inorganic Chemistry*; Wiley-Interscience: New York, 1971; Vol. 14, p 241.
(4) Dreher, M.; Elias, H.; Paulus, H. *Z. Naturforsch., B* **1987**, *42B*, 707.

0020-1669/90/1329-3799$02.50/0

(1), which can be followed and characterized by temperature-

$$\text{planar } (S = 0) \rightleftharpoons \text{tetrahedral } (S = 1) \qquad (1)$$

dependent ^{1}H NMR spectroscopy.[3] There are reports in the literature claiming that the pseudotetrahedral copper complexes $Cu(R\text{-}sal)_2$ are also subject to such a planar $\rightleftharpoons$ tetrahedral structural equilibrium in solution. The arguments for this are derived from dipole moment data[5] and from ^{1}H NMR spectra of $Cu(iPr\text{-}sal)_2$.[6] The finding[7,8] that the ligand field spectra of pseudotetrahedral complexes $Cu(R\text{-}sal)_2$ are essentially the same in the crystalline state and in solution favors the view, however, that the complexes dissolve without structural change and that an equilibrium planar $\rightleftharpoons$ tetrahedral in solution is not involved.

The somewhat ambiguous background to be found in the literature led us to study a series of complexes $Cu(R\text{-}sal)_2$ (I, II, IV–VII) by ligand field[9] and EPR spectroscopy[9] in the solid state

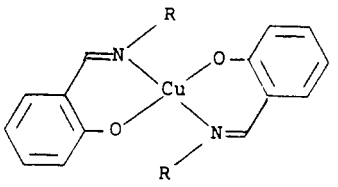

$Cu(R\text{-}sal)_2$

I = $Cu(Me\text{-}sal)_2$; R = $-CH_3$

II = $Cu(Et\text{-}sal)_2$; R = $-CH_2-CH_3$

III = $Cu(nPr\text{-}sal)_2$; R = $-CH_2-CH_2-CH_3$

IV = $Cu(iPr\text{-}sal)_2$; R = $-CH(CH_3)_2$

V = $Cu(neoPe\text{-}sal)_2$; R = $-CH_2-C(CH_3)_3$

VI = $Cu(DMPe\text{-}sal)_2$; R = $-CH(CH(CH_3)_2)_2$

VII = $Cu(tBu\text{-}sal)_2$; R = $-C(CH_3)_3$

as well as in solution.[14] In addition, the rate of ligand substitution according to (2) was measured for complexes I–VII in acetone

$$Cu(R\text{-}sal)_2 + H_2salen \rightarrow Cu(salen) + 2R\text{-}salH \qquad (2)$$

as solvent (H_2salen = *N,N'*-disalicylideneethylenediamine). This kinetic study was undertaken in analogy to the corresponding nickel(II) complexes $Ni(R\text{-}sal)_2$ and $Ni(R_2\text{-}ati)_2$ (=bis(*N,N'*-dialkyl-2-aminotropone iminato)nickel(II)), for which the existence of equilibrium 1 has been well established[3] and which react according to (2) exclusively via the planar configurational isomer, the tetrahedrally distorted one being kinetically inert.[15]

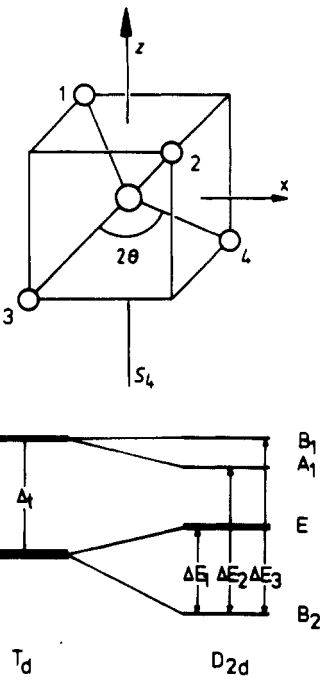

Figure 1. Jahn–Teller distortion of a tetrahedral Cu^{2+} complex ($T_2 \otimes \epsilon$ vibronic coupling) along one S_4 axis and term diagram with possible d–d transitions in T_d and D_{2d} (compression) symmetries. The numbers 1, 2 and 3, 4, respectively, characterize the N and O donor atoms of the two bidentate ligands in complexes $Cu(R\text{-}sal)_2$; 2θ is the mean of the N–Cu–N and O–Cu–O angles. The term sequence of the diagram follows the AOM parameter set in eq 6.

In the present contribution the following questions are raised and dealt with: (i) Is the degree of tetrahedral distortion in the CuN_2O_2 coordination sphere of complexes $Cu(R\text{-}sal)_2$, as observed by X-ray crystallography for the solid state, static or dynamic? (ii) Does the degree of distortion (as found for the solid state) change upon dissolution of complexes $Cu(R\text{-}sal)_2$ in a solvent such as acetone? (iii) Are complexes $Cu(R\text{-}sal)_2$ subject to a dynamic equilibrium planar $\rightleftharpoons$ tetrahedral in solution? (iv) Can the kinetic investigation of ligand substitution according to (2) provide information concerning the existence of equilibrium 1 for complexes $Cu(R\text{-}sal)_2$?

Experimental Section

The solvent acetone (reagent grade, Merck) was used without further purification. The water content of the solvent as determined by Karl Fischer titration was $[H_2O] = 0.04$ M. The ligand H_2salen was obtained according to a published procedure.[15]

Complexes. Complexes I–V and VII were prepared as described earlier.[16,17] The results of elemental analyses were in good agreement with calculated data.

$Cu(DMPe\text{-}sal)_2$ (VI) was prepared in the following way: 5.7 g (0.05 mol) of 3-amino-2,4-dimethylpentane (Ventron) was added dropwise to a solution of 6.1 g (0.05 mol) of salicylaldehyde in 100 mL of MeOH. After several minutes 5.0 g (0.025 mol) of $Cu(AcO)_2 \cdot H_2O$ (dissolved in 100 mL of H_2O) and 5.0 g of NaAcO (dissolved in 50 mL of H_2O) were added. After addition of 2 g (0.05 mol) of NaOH (dissolved in 50 mL of H_2O) the reaction mixture was heated on the steam bath for 30 min. The black-violet crystals formed upon cooling were recrystallized twice from MeOH (mp 148–149 °C). Anal. Calcd: C, 67.24; H, 8.06; N, 5.60. Found: C, 67.25; H, 8.24; N, 5.56.

Electronic Spectra. The near-IR/vis spectra of the solid samples were recorded with a Zeiss PMQ II spectrophotometer equipped with a low-temperature accessory (allowing temperatures as low as 5 K) and an accessory (RA2) for the measurement of the reflection spectra. The reflection data were transformed into absorbance data by using the Schuster–Kubelka–Munk formula. For the near-IR/vis solution spectra

(5) Kogan, V. A.; Osipov, O. A.; Shcherbak, S. N.; Zhuchenko, T. A. *Dokl. Phys. Chem.* **1968**, *181*, 624; *J. Gen. Chem. USSR (Engl. Transl.)* **1968**, *38*, 1556.
(6) Fritz, H. P.; Golla, B. M.; Keller, H. J.; Schwarzhans, K. E. *Z. Naturforsch., B* **1966**, *21B*, 725.
(7) Sacconi, L.; Ciampolini, M. *J. Chem. Soc.* **1964**, 274.
(8) Cheeseman, T. P.; Hall, D.; Waters, T. N. *J. Chem. Soc. A* **1966**, 694.
(9) It should be pointed out that spectroscopic data for some of the copper(II) complexes, particularly in the magnetically diluted solid state, were taken earlier;[10-13] the experimental conditions were somewhat different, however, so that new data had to be collected.
(10) Fritz, H. P.; Golla, B. M.; Keller, H. J. *Z. Naturforsch., B* **1968**, *23B*, 876.
(11) Nonaka, Y.; Tokii, T.; Kida, S. *Bull. Chem. Soc. Jpn.* **1974**, *47*, 312.
(12) Yokoi, H. *Bull. Chem. Soc. Jpn.* **1974**, *47*, 3037.
(13) Wassom, J. R.; Richardson, H. W.; Hatfield, W. E. *Z. Naturforsch, B* **1977**, *32B*, 551.
(14) The time scale for electronic transitions is about 10^{-14} s, while the EPR method is much slower ($\geq 10^{-8}$ s). The inverse frequency for the configurational change from the tetrahedral to the square-planar arrangement as induced by the ϵ-mode in T_d symmetry (see below) is approximately 10^{-13} s. Thus, the electronic spectra reflect the actual geometry, while the information resulting from EPR spectra would describe an averaged situation in the case of a dynamic equilibrium tetrahedral $\rightleftharpoons$ square-planar.
(15) Schumann, M.; Elias, H. *Inorg. Chem.* **1985**, *24*, 3187.
(16) Voss, H.; Wannowius, K. J.; Elias, H. *J. Inorg. Nucl. Chem.* **1974**, *36*, 1402.
(17) Voss, H.; Wannowius, K. J.; Elias, H. *J. Inorg. Nucl. Chem.* **1975**, *37*, 79.

Table I. Selected Crystallographic Data for Complexes Cu(R-sal)$_2$ in the Solid State

complex	R	space group	$\delta(2\theta)$,[a] deg	ref
I	Me	Iba_2	70.5	*b*
II	Et	$P2_1/c$	45 ± 2	*c*
IV	iPr	*Pbca*	28	*d*
VII	tBu	$P2_12_12_1$	32 ± 4	*e*
V	neoPe	$P2_1/c$	70.5	*f*
VI	DMPe	$P2_1/c$	53 ± 2.5	*f*

[a] For definition of 2θ (=O–Cu–O angle), see Figure 1; $\delta(2\theta)$ = difference between 2θ and 109.5° (tetrahedron). [b] Steurer, W.; Adlhart, W. *Acta Crystallogr.* **1983**, *39*, 721. [c] Baker, E. N.; Clark, G. R.; Hall, D.; Waters, T. N. *J. Chem. Soc. A* **1967**, *251*. [d] Reference 24. [e] Cheeseman, T. P.; Hall, D.; Waters, T. N. *J. Chem. Soc. A* **1966**, 685. [f] Reference 23.

a double-beam spectrophotometer (Zeiss DMR 21) was used.

EPR Spectra. The EPR spectra of the solid samples and of the (frozen) solutions were recorded with an EPR spectrophotometer (Varian E15) equipped with a low-temperature accessory (range for the Q band 34.5–35.5 GHz; range for the X band 8.2–9.2 GHz). DPPH was used as internal standard (g_{DPPH} = 2.0037). The EPR spectra of single crystals were taken in the three orthogonal planes in steps of 15°. The single crystal was fixed on a LiF cube along a crystallographic axis with silicone grease.

Kinetic Measurements. The kinetic measurements were done with a diode-array spectrophotometer (HP 8451A) in two-chamber cells (path length 2 × 0.436 cm), the chambers containing the solutions of the copper complex and of the ligand H_2salen, respectively. After thermostating, the cell was taken out of the spectrophotometer and quickly shaken to start the reaction by mixing the solutions. The kinetic runs were carried out under pseudo-first-order conditions ([H_2salen] ≥ 10[complex]) and monitored at 500 nm (Cu(tBu-sal)$_2$) and at 570 nm, respectively. The absorbance/time data were stored, and a total of 60–100 data points were fitted to an exponential function with a computer program on the basis of the least-squares method. The deviation from first-order kinetics was in general less than 1%.

Spectroscopic Results

A. General Background. It is well established that the $T_2(e^4t_2^5)$ ground state of the Cu^{2+} ion in tetrahedral coordination undergoes rather strong vibronic Jahn–Teller coupling with the vibrational ϵ-mode leading from the T_d point group into distinctly tetragonally compressed tetrahedra of D_{2d} symmetry[18,19] (Figure 1). Single-crystal or powder EPR measurements on solid compounds with four-coordinate Cu^{2+} ions usually yield g values that are not or only weakly temperature dependent and that correspond to a B_2 ground state (hole in the d_{xy} orbital) and a static distortion of the kind just mentioned. The orbital contributions u in the perturbation term of eq 3 depend on the covalency parameters k (which

$$g_\parallel = g_o + 8\cdot u_\parallel \qquad u_\parallel = k_\parallel^2\,\lambda_o / \Delta E_3$$
$$g_\perp = g_o + 2\cdot u_\perp \qquad u_\perp = k_\perp^2\,\lambda_o / \Delta E_1 \qquad (3)$$

are essentially orbital reduction factors[20]), on the spin–orbit coupling parameter λ_0 (λ_0 = 830 cm^{-1} for the free Cu^{2+} ion), and on the energies of the d–d transitions in the ligand field spectrum (Figure 1). In order to prove that an observed distortion in the solid state is caused by the Jahn–Teller effect and not induced by crystal packing effects in the unit cell, the comparison with the geometric data of corresponding cobalt(II) and zinc(II) complexes is helpful, since the ionic radii of Co^{2+} and Zn^{2+} are very similar to the radius of Cu^{2+} and since these ions possess Jahn–Teller stable $^4A_2$ and $^1A_1$ ground states, respectively. It has been shown[18,19] that in general the Jahn–Teller coupling mainly controls the distortion of the Cu^{2+} tetrahedra although crystal packing effects cannot be ruled out completely. As compared to the observed distortion in solution, crystal packing may either alter the degree of tetragonal compression of the tetrahedra in either direction and/or induce small deformations to lower symmetry.

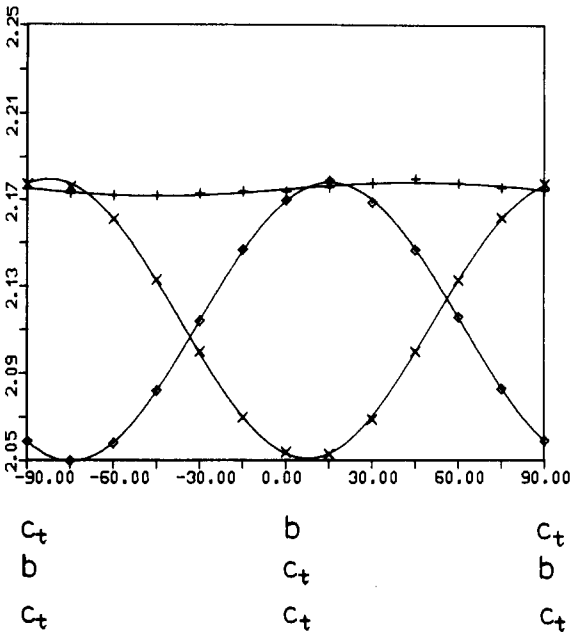

Figure 2. Angular dependence of the g values for the complex Cu(iPr-sal)$_2$. (The crystallographic a axis and c axis could not be discriminated in the crystal morphology, $a \approx c \equiv c_t$.)

Because of their N_2O_2 set of donor atoms complexes, Cu(R-sal)$_2$ complexes possess C_{2v} symmetry only (in the idealized case). Due to the corresponding symmetry reduction $D_{2d} \rightarrow C_{2v}$, a small splitting of the $^2B_2 \rightarrow {}^2E$ transition in the d–d spectra (Figure 1) and of the spectroscopic $g_\perp$ values (eq 3) is expected.

B. Solid-State EPR and Ligand Field Spectra. Structural data for most of the complexes studied are known. The Cu–O distances lie in the narrow range 1.89 ± 0.015 Å, whereas the Cu–N bond lengths vary in the range 1.96 ± 0.05 Å. The axial compression as given by the parameter $\delta(2\theta)$ (see Table I) is less than halfway between T_d geometry ($\delta(2\theta)$ = 0°) and D_{4h} geometry ($\delta(2\theta)$ = 70.5°) for complexes Cu(iPr-sal)$_2$ and Cu(tBu-sal)$_2$ and increases for Cu(Et-sal)$_2$ and Cu(DMPe-sal)$_2$ to arrive at $\delta(2\theta)$ = 70.5° for Cu(Me-sal)$_2$ and Cu(neoPe-sal)$_2$, which are square-planar.

The angular dependence of the observed single-crystal EPR signal of the complex Cu(iPr-sal)$_2$ (293 K, Q-band) is shown in Figure 2. Four of the eight Cu^{2+} polyhedra in the orthorhombic unit cell (*Pbca*)[21] are magnetically nonequivalent but may be grouped into two pairs. The C_2 axes of each pair are equivalently oriented within ±2°, with angles of approximately 45° with respect to the crystallographic a and c axes. On the other hand, the C_2 axes of the two pairs are inclined to the ac plane by ±8°. Their projections into the (010) plane are perpendicularly orientated to each other, however (canting angle 2γ = 90°, antiferrodistortive order[22] of compressed tetrahedra). Since only one EPR signal is observed, exchange coupling between the two magnetically different polyhedra is apparently present (Cu–Cu spacings ≈ 7.5 Å). The molecular **g** tensor is expected to follow the polyhedron symmetry, with the g_z component along the C_2 axis and with g_x and g_y being located in the two molecular σ_v planes. The molecular g values can be calculated from the experimental exchange-coupled g^{ex} values via eq 4 with γ = 45°, if axial symmetry of the CuN_2O_2

$$g_1^{ex} = g_\perp$$
$$g_2^{ex} = g_\perp \cos^2\gamma + g_\parallel \sin^2\gamma$$
$$g_3^{ex} = g_\perp \sin^2\gamma + g_\parallel \cos^2\gamma \qquad (4)$$

polyhedra (D_{2d}) is assumed ($g_z \equiv g_\parallel$; $g_x - g_y = g_\perp$). The angular dependencies of the g^{ex} components in the crystallographic (001), (010), and (100) planes are in agreement with the given analysis

(18) Reinen, D. *Comments Inorg. Chem.* **1983**, *2*, 227.
(19) Reinen, D.; Allmann, R.; Baum, G.; Jakob, B.; Kaschuba, U.; Massa, W.; Miller, G. J. *Z. Anorg. Allg. Chem.* **1987**, *548*, 7.
(20) Stevens, K. W. H. *Proc. R. Soc. London, A* **1953**, *A219*, 542.
(21) Orioli, P. L.; Sacconi, L. *J. Am. Chem. Soc.* **1966**, *88*, 277.
(22) Reinen, D.; Friebel, C. *Struct. Bonding (Berlin)* **1979**, *37*, 1.

Table II. g- and A-Tensor Components for Complexes Cu(R-sal)$_2$

Solid State

complex	T, K	g_x	g_y	g_z	g_{av}
I	298/130	2.04_6		$\approx 2.20_5$	2.09_9
II	298/130/4.2	$(\approx 2.04_0)^a$		$(\approx 2.24_2)^a$	2.10_7
IV	298/77	$(\approx 2.04_9)^a$		$(\approx 2.30_2)^a$	2.13_3
V	298/130	2.03_7	2.05_2	2.21_9	2.10_3
VI	298/130/4.2	$\approx 2.04_3$		2.23_1[c]	2.10_6
VII	298/130	$(\approx 2.05_0)^a$		$(\approx 2.30_5)^a$	2.13_5

Solution

	frozen soln in DMF and acetone (T = 130 K)					soln in acetone (T = 298 K)	
complex	g_x'	g_y'	g_z'	g_{av}'	$10^4 A_z'$,[b] cm^{-1}	$\bar{g}'$	$10^4 \bar{A}'$,[b] cm^{-1}
I	2.05_0		2.24_6	2.11_5	−184	2.11_5	−75
II	2.03_8	2.05_9	2.22_9	2.10_9	−177	2.10_8	−75
IV	$\approx 2.03_8$	2.04_5	2.25_6	2.11_3	−174	2.12_4	−66
V	2.03_8	2.05_7	2.22_6	2.10_7	−180	2.11_3	−74
VI	$\approx 2.04_3$		2.22_8	2.10_5	−187	2.11_3	−71
VII	2.04_9	$\approx 2.06_5$	2.27_3	2.12_9	−146	$\approx 2.13_5$	≈ -42[d]

[a] Calculated from the exchange-coupled $\langle \mathbf{g}^{ex} \rangle$ tensor with the assumption of tetragonal molecular g values ($g_1^{ex} = 2.04_0, 2.04_9, 2.05_0$, $g_2^{ex} = 2.12_0, 2.17_0, 2.14_3$, and $g_3^{ex} = 2.16_2, 2.18_2, 2.21_3$ for R = Et, iPr, and tBu). [b] Hyperfine splittings in g_z' and $\bar{g}'$. [c] $A_z = -161 \times 10^{-4}$ cm^{-1}. [d] Badly resolved.

(Figure 2). Single-crystal EPR data of the complexes Cu(Me-sal)$_2$ and Cu(tBu-sal)$_2$ were analyzed along similar lines (Table II).

The unit cell of the complex Cu(DMPe-sal)$_2$, for which a structure determination was carried out recently,[23] contains two magnetically inequivalent Cu^{2+} polyhedra with a canting angle $2\gamma = 60°$ between the g_z axes, in agreement with the angular dependence of the g values in the single-crystal EPR experiment. They are not exchange coupled because two signals with well-resolved Cu^{2+} hyperfine structure in the g_z direction ($|A_z| = 161 \times 10^{-4}$ cm^{-1}) are observed. This is probably due to the large Cu–Cu distances in the unit cell (approximately 10 Å) as a consequence of the sterically demanding alkyl group in the complex Cu(DMPe-sal)$_2$. From A_z ($\equiv A_\parallel$), assuming a negative sign, a mixing coefficient $\alpha = 0.83$ in the ground-state MO (eq 5; $L_{x^2-y^2}$ = symmetry-adapted linear combination of ligand orbitals) is calculated.[24] The powder g values are identical with those obtained for single crystals within the experimental uncertainties and exhibit no marked temperature dependence (Table II, Figure 3). The unit cells of the complexes Cu(Me-sal)$_2$ and Cu(neoPe-sal)$_2$ contain only one magnetically inequivalent Cu^{2+} polyhedron, and the observed g-tensor components can be considered as reflecting the molecular geometries. They indicate, in agreement with the assumption of nearly tetragonal g values, the presence of only small orthorhombic components. The average g values g_{av} compiled in Table II directly reflect the molecular geometry. For the pseudotetrahedral compounds Cu(iPr-sal)$_2$ and Cu(tBu-sal)$_2$ the value for g_{av} is 2.13_5, whereas $g_{av} \approx 2.10$ is obtained for the square-planar or nearly square-planar complexes.

$$\Psi = \alpha d_{x^2-y^2} - \alpha' L_{x^2-y^2} \quad (5)$$

The ligand field spectra of Cu(iPr-sal)$_2$ and Cu(tBu-sal)$_2$ exhibit two broad bands in the near-IR and vis range at about the same energies, namely 9000 and 13 500 cm^{-1} (Figure 4). In line with flat minima in the vis range at about 16 000 cm^{-1}, the color is brown-red. Nearly equal transition energies are indeed expected because the extent of distortion in both complexes is approximately the same ($2\theta \simeq 140°$; see Table I). Above 16 000 cm^{-1} the charge-transfer bands dominate. The two ligand field bands are

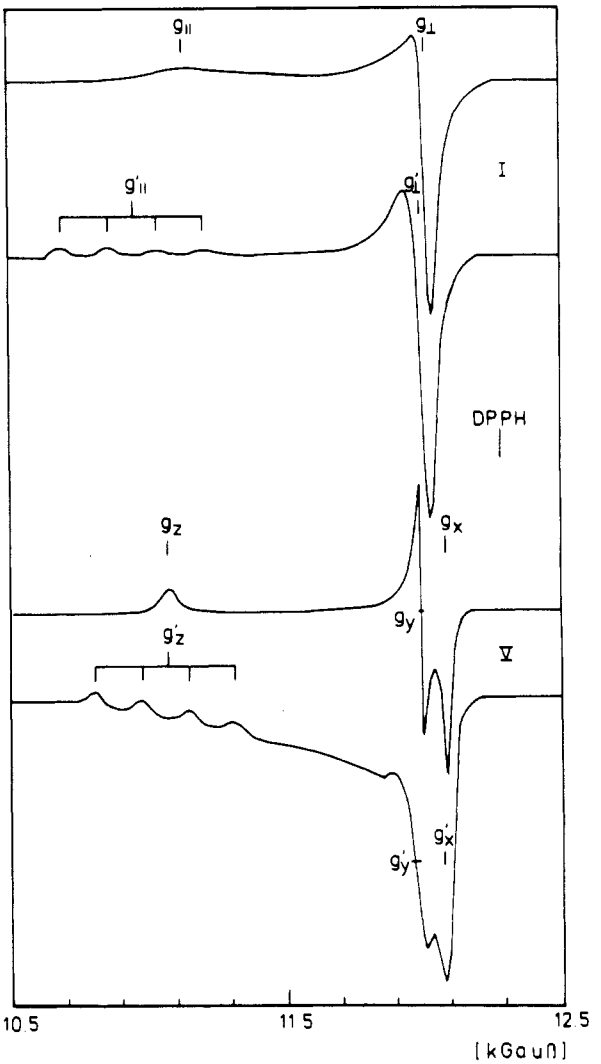

Figure 3. EPR powder spectra at 298 K (top) and frozen-solution spectra at 130 K (bottom) of complexes Cu(Me-sal)$_2$ (I) and Cu(neoPe-sal)$_2$ (V).

assigned to the symmetry-allowed $B_2 \rightarrow E(\Delta E_1)$ and $B_2 \rightarrow A_1(\Delta E_2)$ transitions in D_{2d} and can be reproduced in the angular overlap model (AOM) by the parameter set (6), by applying the

$$e_\sigma = 6000 \text{ cm}^{-1} \qquad e_\pi^\perp \simeq 1000 \text{ cm}^{-1}$$
$$e_{ds} \simeq 1500 \text{ cm}^{-1} \qquad e_{\pi\parallel} \simeq 0 \quad (6)$$

corresponding energy equations,[28] with an O–Cu–O angle of 140°. The anisotropic e_π parameters reflect that π-bonding is possible only perpendicular to the plane of the bidentate ligands, while e_{ds} is due to the s–d_{z^2} interaction.[25] The parameter set of eq 6 depends exclusively on the copper–ligand distances; within certain limits it should hence be valid for all copper(II) complexes under study.

For complexes Cu(Me-sal)$_2$ and Cu(Et-sal)$_2$ the two transitions $^2B_2 \rightarrow {}^2E$ and $^2B_2 \rightarrow {}^2A_1$ are expected at 16 000 and 18 000 cm^{-1} (R = Me) and 13 000 and 15 850 cm^{-1} (R = Et), respectively. In line with this a shoulder around 12 000 cm^{-1} and a broad band at about 16 000 cm^{-1} are observed for the complex Cu(Et-sal)$_2$, whereas for the square-planar complex Cu(Me-sal)$_2$ only one broad band between 16 000 and 18 000 cm^{-1} is observed (Table III). The flat minimum at approximately 18 000 cm^{-1} corresponds to the olive green color of the complexes. The reflection spectrum of complex VI is sufficiently resolved at 5 K only, with a band at $\simeq$14 000 cm^{-1} and an unstructured absorption above 16 000 cm^{-1} (which is in good agreement with $^2B_2 \rightarrow {}^2E$, $^2A_1$ transition

(23) Elias, H.; Paulus, H.; Wannowius, K. J. To be published.
(24) Ozarowski, A.; Reinen, D. *Inorg. Chem.* **1985**, *24*, 3860.
(25) Smith, D. W. *Struct. Bonding (Berlin)* **1972**, *12*, 49.
(26) Ham, F. S. *Phys. Rev.* **1965**, *138*, A1727.
(27) Elias, H.; Fröhn, U.; von Irmer, A.; Wannowius, K. J. *Inorg. Chem.* **1980**, *19*, 869.
(28) Elias, H.; Fröhn, U.; Giegerich, G.; Stenger, M.; Wannowius, K. J. *J. Chem. Soc., Dalton Trans.* **1982**, 577.

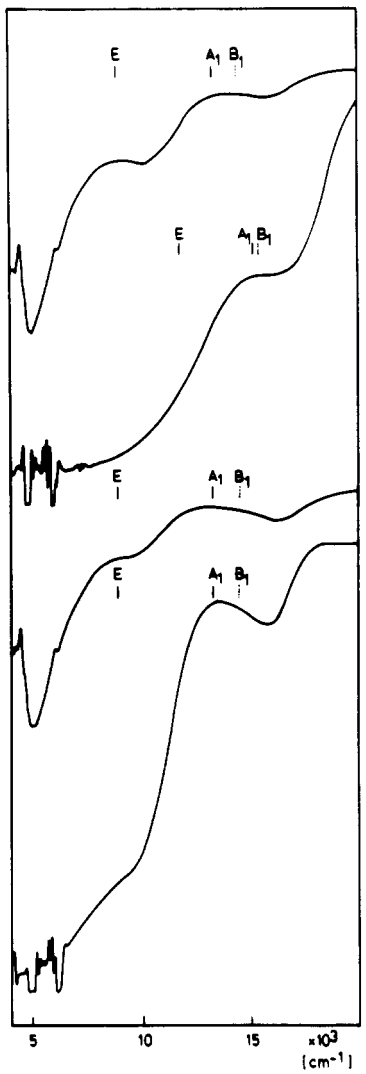

Figure 4. Solid-state reflection spectra at 298 K (top) and solution spectra at 130 K (bottom) of complexes Cu(iPr-sal)$_2$ (IV) (upper two spectra) and Cu(tBu-sal)$_2$ (VII) (lower two spectra). Ligand field transitions were calculated with the parameter set of eq 6 and the structural angles $2\theta = 140°$ (R = iPr, tBu, solid state, (see Table I); R = tBu, solution) and 150° (R = iPr, solution). The fine structure below ≈7000 cm^{-1} is due to N–H and C–H skeleton vibrations and/or the solvent acetone (intensities in arbitrary units).

Table III. Ligand Field Transition Energies for Complexes Cu(R-sal)$_2$ (T = 298 K)

		powder reflectance		acetone soln	
complex	R	$10^{-3}\Delta E_1$,[d] cm^{-1}	$10^{-3}\Delta E_2$,[e] cm^{-1}	$10^{-3}\Delta E_1$,[d] cm^{-1}	$10^{-3}\Delta E_2$,[e] cm^{-1}
I	Me	≈15–18		[c]	≈16.5
II	Et	≈12.0	≈16.0	(≈12)[b]	≈17.0
IV	iPr	9.0	≈14.0	[c]	≈15.5
V	neoPe	14.5	(>16)	13.0	≈16.5
VI	DMPe	14.0[a]	(>16)[a]	[c]	≈16.5
VII	tBu	≈9.0	13.5	≈9.0	13.5

[a] 5 K. [b] Very weak. [c] Not resolved for intensity reasons. [d] Assignment: $^2B_2 \rightarrow {}^2E$ (in D_{2d}). [e] Assignment: $^2B_2 \rightarrow {}^2A_1$ (in D_{2d}).

energies of 14 250 and 16 750 cm^{-1}, as calculated with $\delta(2\theta) = 53°$; see Table I). For the yellow-brown complex Cu(neoPe-sal)$_2$ (V) a planar geometry is found,[23] although the ligand field spectrum (with a well-resolved band at 14 500 cm^{-1} and a continuous increase in absorption at energies above the minimum at 16 000 cm^{-1}) and the g values (Table II) suggest a slight deviation from planarity or a weak additional bonding in the axial positions.

The consistency of the spectral assignment and the AOM description should become apparent also in the g values of the complexes. The covalency factors $k_\parallel$, as deduced from the molecular $g_\parallel$ values (Table II, eq 3) by using calculated energies for the symmetry-forbidden $^2B_2 \rightarrow {}^2B_1$ transition, range indeed from 0.81 for the pseudotetrahedral complexes IV and VII to 0.74 for the square-planar complex I and are hence of the expected magnitude for oxygen or nitrogen donor atoms. The $k_\perp$ values are much lower, indicating a further strong reduction presumably due to the Ham effect.[26]

There is no indication of fluxional behavior in the d–d spectra in the sense of an equilibrium square-planar ⇌ tetrahedral induced by the tetrahedral ε-mode. In addition, the analysis of the structure data for the solid compounds with respect to the thermal ellipsoids of the donor atoms does not provide evidence for dynamic behavior. On the contrary, the structural and spectroscopic data for the solid complexes listed in Tables I and II can be interpreted consistently only if statically distorted tetrahedra are invoked. The degree of this distortion as associated with the alkyl group R and as characterized by the angle 2θ is

$$\text{Me, neoPe (180°)} > \text{DMPe (163°)} > \text{Et (155°)} > \text{tBu (142°)} > \text{iPr (138°)} \quad (7)$$

C. Solution EPR and Ligand Field Spectra. The g values of the complexes obtained for acetone solutions and frozen solutions (DMF and partly acetone) at 130 K are listed in Table II. The d–d transition energies are compiled in Table III. For complex VII (red solution) the solution spectrum is identical with that obtained in the solid state although the band intensities have changed (see Figure 4). In particular the $^2B_2 \rightarrow {}^2E$ transition becomes rather weak. The solid-state g values are slightly larger than those obtained in frozen solution but match nicely with the average g value g'_{av} in solution. Similarly, the EPR and ligand field spectra of complex II change only slightly upon switching from the solid state to the solution. For complex I a considerable decrease of 2θ from 180 to about 155° can be deduced from the EPR data (see Figure 3). The same angle is estimated for complex V. For the switch from the solid state to solution, complex Cu(iPr-sal)$_2$ undergoes a change from $\delta(2\theta) = 28°$ to approximately 40°, as can be estimated from band shifts to higher energies in the electronic spectrum (see Figure 4) as well as from the decrease of the g_{av} values. In the case of complex VI, for which the g_{av}' values and the optical data in solution are identical with those of complexes I and V (see Tables II and III), there is a change of the 2θ value from 163° to about the same angle of approximately 155°.

The g_{av}' values of complexes V and VI are close to g_{av} and differ (see Table II) from those in solution ($\bar{g}'$), which indicates the presence of matrix effects also for the solid solution. Interestingly enough, the solution $\bar{g}'$ value of complex IV lies between the g_{av} value for the solid state and that for the frozen solution. In this case the matrix effects apparently decrease the tetrahedral angle and increase it, respectively, as compared to the geometry in solution.

The overall result concerning the size of the angle 2θ as affected by the alkyl group R in acetone solution is given by the sequence (8). Four of the six complexes have nearly the same geometry

$$180° \gg \text{Et} \gtrsim \text{Me} \approx \text{neoPe} \approx \text{DMPE (≈155°)} > \text{iPr (≈150°)} > \text{tBu (≈140°)} > 109.5° \quad (8)$$

with $2\theta \approx 155°$ in solution, which seems to reflect the Jahn–Teller coupling without disturbance by matrix effects and steric hindrance due to rigid ligands. Complexes IV and VII posses geometries nearer to the undistorted tetrahedron because of steric ligand effects. These are induced by the branching at the α-carbon and are indeed expected to be more effective for complex VII than for complex IV. The position of the DMPe complex in the series (8) is unexpected, since the DMPe-substituted ligand is also α-branched; this will be discussed below. Comparing sequences (7) and (8), one learns that the much more pronounced compression of complexes V and I in the solid state up to the planar limit is obviously a matrix effect.

The mixing coefficient α (see eq 5) as deduced from the well-resolved Cu hyperfine structure constant $A_z' \simeq A_\parallel'$ in the $g_z' \simeq g_\parallel'$ signal of the EPR spectrum of frozen solutions (taken

Table IV. Rate Constants[a] for Ligand Substitution in Complexes $Cu(R\text{-}sal)_2$ According to Reaction 2 in Acetone at 298 K

complex	R	10^3k_S, s^{-1}	10^2k_L, M^{-1} s^{-1}	$K_{p,t}$[b]	K_{py},[c] M^{-1}	$\Delta H^{\ddagger}$,[d] kJ mol^{-1}	$\Delta S^{\ddagger}$,[d] J mol^{-1} K^{-1}
I	Me	3.83 ± 0.54	16.5 ± 0.8	0		39.1 ± 2.7	−128 ± 9
IV	iPr	1.88 ± 0.01	2.04 ± 0.05	7.09	0.21	76.1 ± 7.9[e]	−17 ± 27[e]
III	nPr	0.97 ± 0.12	1.57 ± 0.22	9.51	0.51	42.5 ± 2.6	−137 ± 8
II	Et	1.45 ± 0.01	1.17 ± 0.02	13.1	0.54	42.3 ± 3.6	−134 ± 12
VI	DMPe	0.927 ± 0.003	0.606 ± 0.021	26.2		40.2 ± 2.0	−147 ± 6
VII	tBu	1.10 ± 0.06	0.573 ± 0.109	27.8	0.31	58.4 ± 12.5[e]	−94 ± 42[e]
V	neoPe	0.184 ± 0.005	0.0954 ± 0.0099	172	0.17	57.3 ± 9.2[e]	−118 ± 45[e]

[a] From spectrophotometric measurements at six different concentrations of H_2salen = L in the range $[L]_0$ = 0.001–0.1 M and by fitting of the experimental rate constant k_{obs} to $k_{obs} = k_S + k_L[L]$; $[Cu(R\text{-}sal)_2]_0 = 1 \times 10^{-4}$ M. [b] Calculated from k_L and $k_p = k_L(R = Me) = 16.5$ M^{-1} s^{-1} according to eq 12. [c] Equilibrium constant for pyridine addition in toluene according to eq 15 at 298 K; data from ref 31. [d] From measurements[a] at six different temperatures in the range 290–318 K. The data for $\Delta H^{\ddagger}$ and $\Delta S^{\ddagger}$ refer to rate constant k_L. [e] Large error due to small contribution of $k_L[L]$ to k_{obs}.

at 130 K) is consistently constant ($\alpha = 0.86 \pm 0.02$) and slightly larger than the one measured for the complex $Cu(DMPe\text{-}sal)_2$ in the solid state. From the hyperfine structure in the isotropic $\bar{g}'$ signal of the solution EPR spectra of complexes I, II, and IV–VI taken at 298 K (cf. Table II), α-values were calculated ($\alpha = 0.85 \pm 0.01$) that are nearly identical with those of the frozen solutions and prove the consistency of the interpretation given above.

A temperature dependence of the $\bar{g}'$ and $\bar{A}'$ values obtained from the solution spectra (see Table II; 200–300 K) was not observed. So, the ligand field and EPR spectra do not provide any indication for a dynamic tetrahedral ⇌ square-planar interconversion of complexes $Cu(R\text{-}sal)_2$ in solution.

Kinetic Results

The replacement of the two bidentate ligands in $Cu(R\text{-}sal)_2$ according to eq 2 is presumably a two-step process. The fact that the absorbance/time data cover the full absorbance range expected for reaction 2 and that they can be fitted satisfactorily to a single exponential function leads to the conclusion that loss of the first bidentate ligand is rate controlling, the displacement of the second one being a fast consecutive reaction. The two-term rate law 9

$$\text{rate} = d[Cu(salen)]/dt = (k_S + k_L[H_2salen])[complex] \quad (9)$$

follows from the dependence of the experimental rate constant k_{obs} on the excess concentration of H_2salen. The data obtained for k_S and k_L are compiled in Table IV. As compared to the corresponding nickel complexes $Ni(R\text{-}sal)_2$, for which the ligand-independent rate term $k_S[Ni(R\text{-}sal)_2]$ is negligibly small,[15] the contribution of the term $k_S[Cu(R\text{-}sal)_2]$ to the overall rate of reaction 2 is substantial. It follows from earlier studies in different solvents,[27,28] however, that the first-order rate constant k_S, when observed for an aprotic solvent such as acetone, has to be attributed to the attack of residual water opening a ligand-independent reaction channel, which adds to the second-order pathway induced by the attack of H_2salen on $Cu(R\text{-}sal)_2$. In earlier contributions the mechanism of the ligand-independent k_S pathway, as initiated by attack of alcohol or water, was discussed in detail.[29,27] The occurrence of mass-law retardation effects[30] as produced by the addition of the leaving ligand R-salH is an important aspect in this discussion. It is also important to point out that slight variations in the concentration of residual water indeed effect the size of k_S but not the size of rate constant k_L,[28] which, as shown in the following paragraph, is of central importance for the present study.

As reviewed by Holm and O'Connor,[3] there are several papers describing the existence of a fast configurational equilibrium planar ⇌ tetrahedra in chloroform for complexes $Ni(R\text{-}sal)_2$ and $Ni(R_2\text{-}ati)_2$ (=bis(*N*,*N*′-dialkyl-2-aminotropone iminato)nickel(II)). In an earlier contribution we determined equilibrium constant $K_{p,t}$ for (10) for a series of complexes $Ni(R_2\text{-}ati)_2$ in acetone and were

$$Ni(R_2\text{-}ati)_2 \text{ (planar)} \overset{K_{p,t}}{\rightleftharpoons} Ni(R_i\text{-}ati)_2 \text{ (tetrahedral)} \quad (10)$$

able to show[15] that second-order rate constant k_L describing second-order ligand substitution according to (11) can be correlated with $K_{p,t}$. This correlation implies that reaction 11 occurs exclusively via the planar isomer of complexes $Ni(R_2\text{-}ati)_2$, the tetrahedral one being kinetically inert under the conditions applied. From the point of formal kinetics this means that second-order rate constant k_L obtained experimentally obeys the relationship (12) with k_p representing the second-order rate constant for the

$$Ni(R_2\text{-}ati)_2 + H_2salen \rightarrow Ni(salen) + 2R_2\text{-}atiH \quad (11)$$

$$k_L = k_p/(1 + K_{p,t}) \quad (12)$$

reaction of H_2salen with the *planar* isomer of $Ni(R_2\text{-}ati)_2$. When inserted in eq 12, the experimental data obtained for k_L and $K_{p,t}$ for complexes $Ni(R_2\text{-}ati)_2$ with R = Me, Et, nPr, All, and Ph indeed result[15] in a mean of $\bar{k}_p = 7 \pm 5$ M^{-1} s^{-1}, with $K_{p,t}$ ranging from 0.018 (R = Me) to 140 (R = Et) and k_L from 4.35 (R = Me) to 0.028 M^{-1} s^{-1} (R = Et).

Assuming that complexes $Cu(R\text{-}sal)_2$ are also subject to a configurational equilibrium analogous to (10), the kinetic analysis carried out for complexes $Ni(R_2\text{-}ati)_2$, as applied to complexes $Cu(R\text{-}sal)_2$, would allow one to calculate hypothetical values for $K_{p,t}$ from the data for k_L on the basis of eq 12, if rate constant k_p were known. Since the sterically least hindered complex $Cu(Me\text{-}sal)_2$ was shown to be rather close to planar geometry in solution (see discussion above), it is reasonable to assume that $k_p \approx k_L$ (R = Me). On the basis of this assumption, one obtains relative data for $K_{p,t}$ (see Table IV) that are not at all in line with the structural information coming from crystallography, EPR spectroscopy, and absorption spectroscopy (see above). This kinetic analysis would make the complex $Cu(neoPe\text{-}sal)_2$ the most tetrahedral one ($K_{p,t}$ = 172), which contradicts the spectroscopic findings. On the contrary, the analysis of the solution spectra puts $Cu(neoPe\text{-}sal)_2$ and complexes $Cu(R\text{-}sal)_2$ with R = Et, Me, and DMPe into the same category of rather planar complexes (see the sequence (8)). So, these results do not provide evidence for the existence of an equilibrium planar ⇌ tetrahedral in the case of complexes $Cu(R\text{-}sal)_2$.

The differences in the size of k_L observed for complexes $Cu(R\text{-}sal)_2$ are interesting though and have to be explained. Considering the spectroscopic findings, the structure of the alkyl groups R attached to the donor nitrogen in complexes $Cu(R\text{-}sal)_2$, and the mechanism of the second-order ligand substitution described by k_L, one is led to steric arguments concerning the accessibility of the copper in $Cu(R\text{-}sal)_2$. Mechanistically, the second-order reaction between $Cu(R\text{-}sal)_2$ and H_2salen is most reasonably described by assuming a fast preequilibrium (13) prior to ligand

$$Cu(R\text{-}sal)_2 + H_2salen \overset{K}{\rightleftharpoons} Cu(R\text{-}sal)_2,H_2salen \quad (13)$$

$$Cu(R\text{-}sal)_2,H_2salen \xrightarrow{k} Cu(salen) + 2R\text{-}salH \quad (14)$$

substitution according to (14). The adduct formed between $Cu(R\text{-}sal)_2$ and H_2salen could possibly be a five-coordinate copper(II) species, since it is well-known[31] that complexes $Cu(R\text{-}sal)_2$

(29) Elias, H.; Hasserodt-Taliaferro, Chr.; Hellriegel, L.; Schönherr, W.; Wannowius, K. J. *Inorg. Chem.* **1985**, *24*, 3192.
(30) Elias, H.; Reiffer, U.; Schumann, M.; Wannowius, K. J. *Inorg. Chim. Acta* **1981**, *53*, L65.
(31) Ewert, A.; Wannowius, K. J.; Elias, H. *Inorg. Chem.* **1978**, *17*, 1691.
(32) Reinen, D.; Atanasov, M.; Nikolov, G. St.; Steffens, F. *Inorg. Chem.* **1988**, *27*, 1678.

tend to add one molecule of pyridine according to (15). On the

$$Cu(R\text{-sal})_2 + py \overset{K_{py}}{\rightleftharpoons} Cu(R\text{-sal})_2 \cdot py \qquad (15)$$

basis of eqs 13 and 14, the experimentally obtained rate constant k_L should follow the concentration of H_2salen in a nonlinear fashion, namely $k_L = kK/(1 + K[H_2\text{salen}])$. The fact that this type of dependence was not observed experimentally even at high concentrations of H_2salen can be taken as an indication for K being very small, so that $k_L = kK$. This means that rate constant k_L is controlled by the size of both k and K and that the activation parameter $\Delta H^{\ddagger}$ (see Table IV) derived from the temperature dependence of k_L does not describe the energy barrier of an elementary step. It is noteworthy, however, that the data obtained for $\Delta S^{\ddagger}$ are all negative, which is in line with steps (13) and (14), i.e., with the associative character of ligand replacement of Cu(R-sal)$_2$ via the ligand pathway characterized by rate constant k_L.

As reflected by the data for K_{py} (see Table IV), the formation of a five-coordinate species is clearly affected by the nature of the group R in complexes Cu(R-sal)$_2$ in a 2-fold sense. Branching at the α-carbon like in R = iPr and tBu obviously shifts the compressed planar geometry distinctly toward the undistorted tetrahedron, which makes the copper less accessible for donor molecules such as pyridine to become coordinated. Another kinetically relevant "shielding effect" appears to be produced, however, by β-branching like in R = neoPe, which does not affect the coordination geometry in solution though (see eq 8). In an alkyl group like R = DMPe both α-branching and β-branching contribute to make the copper less accessible. Since the coordination of H_2salen according to eq 13 is sterically by far more demanding than the coordination of pyridine according to eq 15, the accessibility of the copper in complexes Cu(R-sal)$_2$ could well be the crucial factor in controlling the rate of ligand substitution. This would mean that rate constant $k_L = kK$ is possibly more affected by the size of K than by the size of k.

Discussion and Conclusions

A band in the low-energy region of the d–d spectra (due to the $^2T_2 \rightarrow {}^2E$ transition in a hypothetical tetrahedral configuration and expected around 7500 cm^{-1}) is never observed. The experimental evidence consistently supports the interpretation that there are fixed intermediate configurations, lying between the limiting tetrahedral and square-planar geometries, also in solution.

The geometry of the complex Cu(Me-sal)$_2$ in solution is expected to reflect the Jahn–Teller distortion without significant steric hindrance imposed by the alkyl group R. Apparently the ground-state potential surface along the tetrahedral/square-planar distortion coordinate is flat in this case, because a large increase in 2θ by about 25° is observed for the solid state, which is obviously due to packing forces. On the other hand, the spherelike and sterically demanding *tert*-butyl group in Cu(tBu-sal)$_2$ interferes with the neighboring donor oxygen and stabilizes a 2θ angle that is much closer to that of the undistorted tetrahedron. The complex Cu(iPr-sal)$_2$ is expected to have an intermediate position between Cu(Me-sal)$_2$ and Cu(tBu-sal)$_2$—in agreement with the sequence (8)—while the ethyl group obviously does not introduce any additional steric effect as compared to the methyl group. The very extended and flexible group DMPe in Cu(DMPe-sal)$_2$, which is α-branched as well as β-branched, is expected to induce a strong DMPe–DMPe interference in tetrahedral geometry, which may explain the comparatively large 2θ angle. The existence of an interference of this kind is also supported by the sequence (7), because solid-state packing effects shift 2θ for Cu(iPr-sal)$_2$ from about 150 to 138°, while Cu(DMPe-sal)$_2$ undergoes even a small 2θ change in the opposite direction. It is, therefore, concluded that the sequence (8) is essentially determined by the superposition of the Jahn–Teller effect and steric hindrance of the two types mentioned.

In accounting for the structural properties of complexes Cu(R-sal)$_2$, one has to consider the following two steric effects besides the vibronic Jahn–Teller coupling—if solid-state packing influence is not involved:

(i) Distortion of the CuN_2O_2 polyhedron as a consequence of the steric demands of the alkyl group R and increasing branching at the α-carbon lead to a decrease in the twisting angle 2θ according to the sequence (16) ("R–O" interaction).

$$Me \approx Et > iPr > tBu \qquad (16)$$

(ii) Extended branching at the β-carbon as in the case of DMPe-sal causes a shielding of the axial positions of copper and introduces a second kind of steric interaction by ligand–ligand interference, which is strongest in T_d symmetry ("R–R" interference). The geometry of the complex Cu(DMPe-sal)$_2$ in solution is the same as for the compounds with R = Me, Et, and neoPe, although a decrease of 2θ is expected due to the branching at the α-carbon, as discussed above.

In a comparison of the properties of the $3d^9$ complexes Cu(R-sal)$_2$ and of the $3d^8$ complexes Ni(R-sal)$_2$, the most prominent difference is the dynamic equilibrium (1) found for the nickel complexes[3] and the static distortion found for the copper complexes. The stereochemistry of four-coordinate Cu^{2+} is characterized by usually strongly compressed tetrahedra with widely varying 2θ angles, extending up to the limit of a planar coordination. In the case of Ni^{2+} tetragonally *elongated* tetrahedra are expected as the consequence of the Jahn–Teller coupling in the $^3T_1(e^4t_2^4)$ ground state. In the presence of strong ligands, however, the Jahn–Teller effect in the first excited ^1E state in T_d symmetry may dominate, leading to a square-planar coordination.[30] In line with these considerations, four-coordinate Ni^{2+} is frequently found with T_d symmetry (where the Jahn–Teller distortion is suppressed by spin–orbit coupling)[30] or in the anticipated tetragonally elongated conformation. More common are square-planar complexes, however, in which Ni^{2+} is low-spin configurated. The two limiting T_d and D_{4h} coordinations are well separated from each other in this case, and intermediate configurations are not stable as they are in the case of Cu^{2+}. This is probably the reason that for copper(II) a static, nondynamic distortion is found in contrast to the dynamic equilibrium between the square-planar and tetrahedral configurations observed for nickel(II).

The kinetic data describing ligand substitution according to (2) via the ligand-dependent second-order pathway do also not provide any convincing information supporting the existence of equilibrium 17 in solution. A formal kinetic analysis, which can be successfully

$$Cu(R\text{-sal})_2 \quad (\text{planar}) \overset{K_{p,t}}{\rightleftharpoons} Cu(R\text{-sal})_2 \quad (\text{tetrahedral}) \qquad (17)$$

applied to corresponding nickel complexes,[15] produces data for $K_{p,t}$ that contradict the spectroscopic findings. The mechanistic interpretation of second-order rate constant k_L is in line with the formation of a five-coordinate adduct between Cu(R-sal)$_2$ and H_2salen in a fast preequilibrium. The steric demands of the alkyl group R and its shielding effects obviously control this equilibrium and, hence, the rate of substitution.

Acknowledgment. We thank the Deutsche Forschungsgemeinschaft and the Verband der Chemischen Industrie e.V. for support. Salicyladehyde was kindly provided by Bayer AG, Leverkusen, FRG.